

# Controllable quantum scars in semiconductor quantum dots

J. Keski-Rahkonen,<sup>1</sup> P. J. J. Luukko,<sup>2</sup> L. Kaplan,<sup>3</sup> E. J. Heller,<sup>4</sup> and E. Räsänen<sup>1,4</sup>

<sup>1</sup>Laboratory of Physics, Tampere University of Technology, Finland

<sup>2</sup>Max Planck Institute for the Physics of Complex Systems, Dresden, Germany

<sup>3</sup>Department of Physics and Engineering Physics, Tulane University, New Orleans, USA

<sup>4</sup>Department of Physics, Harvard University, Cambridge, USA

(Dated: March 5, 2022)

Quantum scars are enhancements of quantum probability density along classical periodic orbits. We study the recently discovered phenomenon of strong, perturbation-induced quantum scarring in the two-dimensional harmonic oscillator exposed to a homogeneous magnetic field. We demonstrate that both the geometry and the orientation of the scars are fully controllable with a magnetic field and a focused perturbative potential, respectively. These properties may open a path into an experimental scheme to manipulate electric currents in nanostructures fabricated in a two-dimensional electron gas.

## I. INTRODUCTION

Quantum scars<sup>1,2</sup> are tracks of enhanced probability density in the eigenstates of a quantum system. They occur along short unstable periodic orbits (POs) of the corresponding chaotic classical system. While being an interesting example of the correspondence between classical and quantum mechanics, quantum scars also show how quantum mechanics may suppress classical chaos and make certain systems more accessible for applications. In particular, the enhanced probability density of the scars provides a path for quantum transport across an otherwise chaotic system.

A new type of quantum scarring was recently discovered by some of the present authors.<sup>3</sup> It was found that local perturbations (potential “bumps”) on a two-dimensional (2D), radially symmetric quantum well produce high-energy eigenstates that contain scars of short POs of the corresponding *unperturbed* (without bumps) system. Even though similar in appearance to ordinary quantum scars, these scars have a fundamentally different origin. They result from resonances in the unperturbed classical system, which in turn create semiclassical near-degeneracies in the unperturbed quantum system. Localized perturbations then form scarred eigenstates from these near-degenerate “resonant sets” because the scarred states effectively extremize the perturbation. These perturbation-induced (PI) scars are unusually strong compared to ordinary scars, to the extent that wave packets can be transported through the perturbed system, along the scars, with higher fidelity than through the unperturbed system, even with *randomly placed* perturbations.<sup>3</sup>

In this work we study these perturbation-induced scars in a 2D quantum harmonic oscillator exposed to a perpendicular, homogeneous magnetic field. This system has direct experimental relevance as it is a prototype model for semiconductor quantum dots in the 2D electron gas.<sup>4</sup> Previous studies combining experiments and theory have confirmed the validity of the harmonic approximation to model the external confining potential of

electrons in the quantum dot, up to the quantum Hall regime reached with a strong magnetic field.<sup>5,6</sup> Furthermore, the role of external impurities in 2D quantum dots has been quantitatively identified through the measured differential magnetoconductance that displays the quantum eigenstates.<sup>7</sup> We show that once perturbed by Gaussian impurities, the high-energy eigenstates of the system are strongly scarred by POs of the unperturbed system, and the shape of these scars can be conveniently tuned via the magnetic field. Furthermore, in the last part of the work we replace the impurities with a single perturbation, representing a controllable nanotip,<sup>8</sup> and use the “pinning” property of the scars to control the scars with the nanotip. Together, these methods of controlling the strong, perturbation-induced scars could be used to coherently modulate quantum transport in nanoscale quantum dots.

## II. MODEL SYSTEM

All values and equations below are given in atomic units (a.u.). The Hamiltonian for a perturbed 2D quantum harmonic oscillator is

$$H = \frac{1}{2}(-i\nabla + \mathbf{A})^2 + \frac{1}{2}\omega_0^2 r^2 + V_{\text{imp}}, \quad (1)$$

where  $\mathbf{A}$  is the vector potential of the magnetic field. We set the confinement strength  $\omega_0$  to unity for convenience and assume the magnetic field  $\mathbf{B}$  is oriented perpendicular to the 2D plane. We model the perturbation  $V_{\text{imp}}$  as a sum of Gaussian bumps with amplitude  $M$ , that is,

$$V_{\text{imp}}(\mathbf{r}) = \sum_i M \exp\left[-\frac{(\mathbf{r} - \mathbf{r}_i)^2}{2\sigma^2}\right].$$

We focus on the case where the bumps are positioned randomly with a uniform mean density of two bumps per unit square. In the energy range considered here,  $E = 50 \dots 100$ , hundreds of bumps exist in the classically allowed region. The full width at half maximum (FWHM) of the Gaussian bumps  $2\sqrt{2 \ln 2} \sigma$  is 0.235,

which is comparable to the local wavelength of the eigenstates considered. The amplitude of the bumps is set to  $M = 4$ , which causes strong PI scarring in this energy regime.

We solve the eigenstates of the Hamiltonian of Eq. (1) using the `itp2d` code.<sup>9</sup> This code utilizes the imaginary time propagation method, which is particularly suited for 2D problems with strong perpendicular magnetic fields because of the existence of an exact factorization of the exponential kinetic energy operator in a magnetic field.<sup>10</sup> The eigenstates and energies can be compared to the well-known solutions of a unperturbed system. The unperturbed energies correspond to the Fock-Darwin (FD) spectrum,<sup>11</sup>

$$E_{k,l}^{\text{FD}} = (2k + |l| + 1)\sqrt{1 + \frac{1}{4}B^2} - \frac{1}{2}lB, \quad (2)$$

where  $k \in \mathbb{N}$  and  $l \in \mathbb{Z}$ . In the limit  $B \rightarrow \infty$ , the states condensate into Landau levels. The FD spectrum is observed experimentally in semiconductor quantum dots (see, e.g., Ref. 12).

Before considering further the quantum solutions of the Hamiltonian we briefly discuss the corresponding classical system. The unperturbed 2D harmonic oscillator in a perpendicular magnetic field is analytically solvable as described in the Appendix and Ref. 13. The POs are associated with classical resonances where the oscillation frequencies of the radial and the angular motion are commensurable. In the following, the notation  $(v_\theta, v_r)$  refers to a resonance where the orbit circles the origin  $v_\theta$  times in  $v_r$  radial oscillations. The resonances occur only at certain values of the magnetic field given by

$$B = \frac{v_r/v_\theta - 2}{\sqrt{v_r/v_\theta - 1}}. \quad (3)$$

By classical simulations using the `bill2d` program<sup>14</sup> we have confirmed that a perturbation with amplitude  $M = 4$  is sufficient to destroy classical long-term stability in the system. Any remaining structures in the otherwise chaotic Poincaré surface of a section are vanishingly small compared to  $\hbar = 1$ .

### III. QUANTUM SCARS

Next we describe the quantum solutions of the system. To visualize the spectrum of a few thousand lowest energies as a function of  $B$  we show in Fig. 1 the density of states (DOS) computed as a sum of the states with a Gaussian energy window of 0.001 a.u. The upper and lower panel correspond to the perturbed (with bumps) and unperturbed system, respectively. The  $B$  values indicating resonances  $(v_\theta, v_r)$  are marked by dashed vertical lines. The upper panel of Fig. 1 shows that the bumps are sufficiently weak to not completely destroy the FD degeneracies.

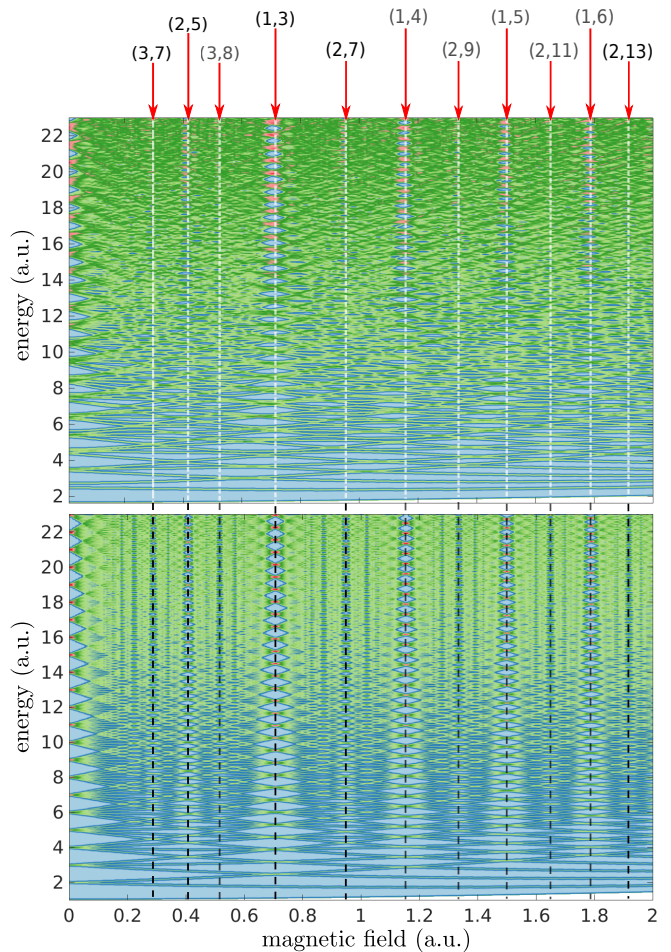


FIG. 1. Scaled (arb. units) density of states (DOS) as a function of the magnetic field for an unperturbed (lower panel) and perturbed (upper panel) two-dimensional harmonic oscillator. The dashed vertical lines indicate the resonances  $(v_\theta, v_r)$  that correspond to a substantial abundance of scarred eigenstates in the perturbed case (see Fig. 2).

As expected from the theory of PI scarring, the eigenstates of the perturbed system show clear scars corresponding to the POs of the unperturbed system. Because of the classical resonance condition (3) these scars appear at specific values of the magnetic field where short classical periodic orbits are possible. Examples of the scars are shown in Fig. 2. The eigenstate number varies between 400...3900. The proportion of strongly scarred states among the eigenstates varies from 10% to 60% at bump amplitude  $M = 4$ . The proportion and strength of scarred states depend on the degree of degeneracy in the spectrum: more and stronger scars appear when more energy levels are (nearly) crossing. The specific shape of the scar for a chosen resonance  $(v_\theta, v_r)$  depends on the energy. For example, the two examples shown for the triangular geometry (1,3) in Fig. 2 correspond to orbits with opposite directions, which are not equivalent because the magnetic field breaks time-reversal symmetry.

As pointed out in Ref. 3, because the scarred states

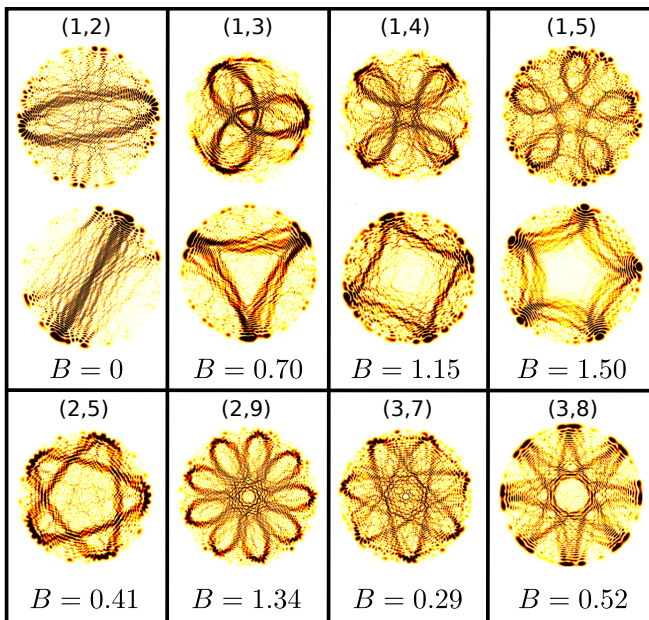


FIG. 2. Examples of scars in a perturbed two-dimensional harmonic oscillator in a magnetic field. The geometries of the scars can be attributed to the classical resonances ( $v_\theta$ ,  $v_r$ ) and the corresponding periodic orbits in the unperturbed system.

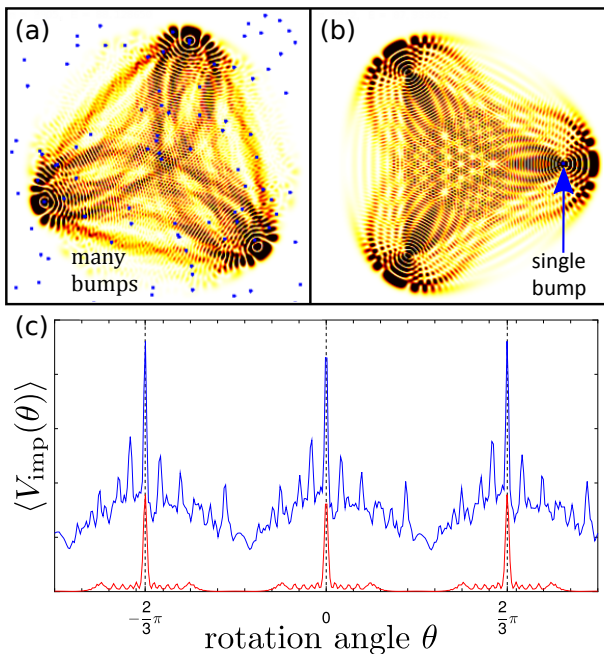


FIG. 3. (a)-(b) Examples of scarred eigenstates at  $B \approx 0.7$  found in a system with several impurities and a single impurity with  $M = 4$ , respectively. The locations and FWHMs of the impurities are denoted with blue dots. (c) Overlap between the scarred state and the impurity potential,  $\langle \psi | V_{\text{imp}}(\theta) | \psi \rangle$ , as a function of the rotation angle with respect to the original orientation  $V_{\text{imp}}$ . The upper (blue) and lower (red) curves correspond to the situations in (a) and (b), respectively. The lower curve has been multiplied by a factor of six for visibility.

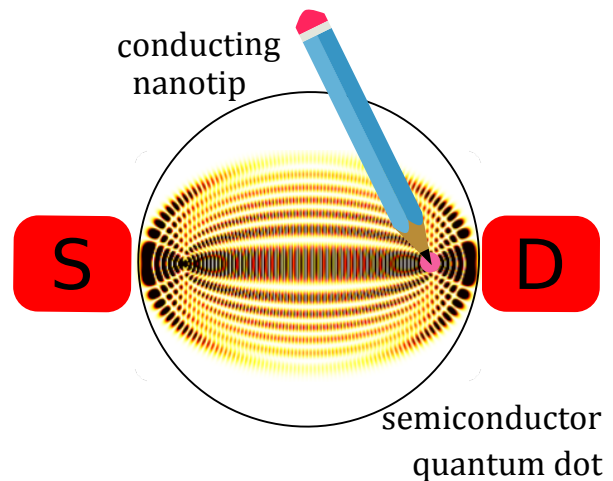


FIG. 4. Schematic figure on the utilization of scars in nanostructures. The magnetic field (here  $B = 0$ ) determines the geometry of the scar (here linear), the energy range refines the geometry further (here longitudinal), and an external voltage gate generates a local perturbation (here the pink dot) that pins the scar, thus determining the orientation.

maximize the perturbation  $V_{\text{imp}}$  they are oriented to coincide with as many bumps as possible. This “pinning” effect is demonstrated in Fig. 3(a). Even a *single* perturbation bump can produce a strong scar that is pinned to its location, as illustrated in Fig. 3(b).

As another view on the pinning effect, Fig. 3(c) shows the overlap between the scarred state and the impurity potential,  $\langle \psi | V_{\text{imp}}(\theta) | \psi \rangle$ , as a function of the rotation angle with respect to the original orientation  $V_{\text{imp}}$ . This is shown for both the multiple-bump (upper curve) and the single-bump (lower curve) cases, corresponding to situations in Figs. 3(a) and (b), respectively. The three distinctive maxima in both cases confirm that the scar is pinned to a location that maximizes the perturbation.

By creating a single perturbation with, e.g., a conducting nanotip,<sup>8</sup> the pinning effect can be used to force the scars to a specific orientation. Together, the magnetic field and the pinning effect provide complete external control over the strength, shape, and orientation of the scars. By selecting which parts of the system are connected by the scar paths, this provides a method to modulate quantum transport in nanostructures in a scheme depicted in Fig. 4. A successful experiment requires that the system is otherwise clean from external impurities such as migrated ions from the substrate.<sup>7</sup> In addition, a sufficient energy range in transport is required as the scars are more abundant at high energies (level number  $\gtrsim 500$ ). In the future, we will study this effect in more detail using realistic quantum transport calculations.

#### IV. SUMMARY

To summarize, we have shown that perturbation-induced quantum scars are found in a two-dimensional harmonic oscillator exposed to an external magnetic field. The scars are relatively strong, and their abundance and geometry can be controlled by tuning the magnetic field. By controlling the orientation of the scars through their tendency to “pin” to the local perturbations, we reach perfect control of the scarring using external parame-

ters. This scheme, using a conducting nanotip as the pinning impurity, may open up a path into “scartronics”, where scars are exploited to coherently control quantum transport in nanoscale quantum systems.

#### V. ACKNOWLEDGMENTS

We are grateful to Janne Solanpää for useful discussions. This work was supported by the Academy of Finland. We also acknowledge CSC – Finnish IT Center for Science for computational resources.

- 
- <sup>1</sup> E. J. Heller, *Phys. Rev. Lett.* **53**, 1515-1518 (1984).
  - <sup>2</sup> L. Kaplan, *Nonlinearity* **12**, R1 (1999).
  - <sup>3</sup> P. J. J. Luukko, B. Drury, A. Klales, L. Kaplan, E. J. Heller, and E. Räsänen, *Sci. Rep.* **6**, 37656 (2016).
  - <sup>4</sup> S. M. Reimann and M. Manninen, *Rev. Mod. Phys.* **74**, 1283 (2002).
  - <sup>5</sup> E. Räsänen, H. Saarikoski, A. Harju, M. Ciorga, and A. S. Sachrajda, *Phys. Rev. B* **77**, 041302(R) (2008).
  - <sup>6</sup> M. C. Rogge, E. Räsänen, and R. J. Haug, *Phys. Rev. Lett.* **105**, 046802 (2010).
  - <sup>7</sup> E. Räsänen, J. Könemann, R. J. Haug, M. J. Puska, and R. M. Nieminen, *Phys. Rev. B* **70**, 115308 (2004).
  - <sup>8</sup> A. C. Bleszynski, F. A. Zwanenburg, R. M. Westervelt, A. L. Roest, E. P. A. M. Bakkers, and L. P. Kouwenhoven, *Nano Lett.* **7**, 2559 (2007); E. E. Boyd, K. Storm, L. Samuelson, and R. M. Westervelt, *Nanotechnology* **22**, 185201 (2011); T. Blasi, M. F. Borunda, E. Räsänen, and E. J. Heller, *Phys. Rev. B* **87**, 241303 (2013).
  - <sup>9</sup> P. J. J. Luukko and E. Räsänen, *Comp. Phys. Comm.* **184**, 769 (2013).
  - <sup>10</sup> M. Aichinger, S. A. Chin, and E. Krotscheck, *Comput. Phys. Commun.* **171**, 197 (2005).
  - <sup>11</sup> V. Fock, *Z. Phys.* **47**, 446 (1928); C. G. Darwin, *Proc. Cambr. Philos. Soc.* **27**, 86 (1930).
  - <sup>12</sup> S. Raymond, S. Studenikin, A. Sachrajda, Z. Wasilewski, S. J. Cheng, W. Sheng, P. Hawrylak, A. Babinski, M. Potemski, G. Ortner, and M. Bayer, *Phys. Rev. Lett.* **92**, 187402 (2004).
  - <sup>13</sup> G. L. Kotkin and V. G. Serbo, *Collection of Problems in Classical Mechanics* (Pergamon Press Ltd., 1971).
  - <sup>14</sup> J. Solanpää, P. J. J. Luukko, and E. Räsänen, *Comp. Phys. Comm.* **199**, 133 (2016).

#### Appendix A: Classical periodic orbits of a two-dimensional harmonic oscillator in a perpendicular and homogeneous magnetic field

Here we present the solution of the equations of motion for a classical particle in a harmonic potential with a perpendicular, homogeneous magnetic field  $B$  [see also G. L. Kotkin and V. G. Serbo, *Collection of Problems in Classical Mechanics* (Pergamon Press Ltd., 1971)]. After choosing the vector potential as  $A_\phi = \frac{1}{2}Br$ , the system

is described, in polar coordinates, by the Lagrangian

$$L = \frac{1}{2}(\dot{r}^2 + r^2\dot{\phi}^2) - \frac{1}{2}\omega_0^2 r^2 + \frac{1}{2}Br^2\dot{\phi}.$$

Its constants of motion are the energy  $E$  and the angular momentum  $p_\phi$ .

In a rotating frame with  $\theta = \phi + \frac{1}{2}Bt$ , the Lagrangian has the form of a simple harmonic oscillator,

$$L = \frac{1}{2}(\dot{r}^2 + r^2\dot{\theta}^2) - \frac{1}{2}\tilde{\omega}^2 r^2,$$

where the effective frequency is

$$\tilde{\omega} = \sqrt{\omega_0^2 + \frac{1}{4}B^2}.$$

Thus, the system is reduced to a harmonic oscillator without a magnetic field, the solution of which can be found in standard texts on classical mechanics [e.g., H. Goldstein, *Classical Mechanics*, 2nd ed. (Addison-Wesley, 1980)]. When the initial conditions are chosen as  $\phi(0) = 0$  and  $r(0) = a$ , the solution in the original coordinates  $(r, \phi)$  is

$$r^2 = a^2 \cos^2(\tilde{\omega}t) + b^2 \sin^2(\tilde{\omega}t)$$

and

$$\phi(t) = -\frac{1}{2}Bt + \arctan\left[\frac{a}{b} \tan(\tilde{\omega}t)\right],$$

where the branches of the arctangent are chosen such that the angle  $\phi$  is a continuous function of time  $t$ . The maximum and minimum radii,  $a$  and  $b$ , are determined by the angular momentum  $p_\phi = \tilde{\omega}ab$  and the energy

$$E = \frac{1}{2}\tilde{\omega}^2(a^2 + b^2) - \frac{1}{2}p_\phi B.$$

The solution shows that the period of radial oscillations  $T = \pi/\tilde{\omega}$  is independent of  $E$  and  $p_\phi$ . The angle with which the radius vector turns during a period is

$$\Delta\phi = \pi\left[\xi(p_\phi) - \frac{B}{2\tilde{\omega}}\right], \quad (\text{A1})$$

where the step function  $\xi(x)$  is

$$\xi(x) = \begin{cases} -1 & \text{if } x < 0 \\ 0 & \text{if } x = 0 \\ 1 & \text{if } x > 0. \end{cases}$$

Note that  $\Delta\phi$  is also independent of  $E$ .

The orbit is periodic exactly when  $\Delta\phi$  is a rational multiple of  $2\pi$ . Other orbits are quasiperiodic. When  $\Delta\phi = 2\pi v_\theta/v_r$ , the particle returns to its initial state after rotating  $v_\theta$  times around the origin and oscillating  $v_r$  times between the radial turning points. Thus, the

classical oscillation frequencies are said to be in  $v_\theta : v_r$  resonance for this particular PO.

By solving Eq. (A1) for the magnetic field, we can determine which value of  $B$  is required for a  $v_\theta : v_r$  resonance. This gives, after elementary algebra, the resonance condition

$$B = \frac{v_r/v_\theta - 2}{\sqrt{v_r/v_\theta - 1}}.$$